Environmental Science and Pollution Research (2019) 26:14339–14349
https://doi.org/10.1007/s11356-019-04611-6

RESEARCH ARTICLE

Thermodynamic and kinetic insights into plant-mediated detoxification of lead, cadmium, and chromium from aqueous solutions by chemically modified *Salvia moorcroftiana* leaves

Syed Muhammad Salman[1] · Asad Ali[1,2] · Behramand Khan[1] · Mehmood Iqbal[3] · Muhammad Alamzeb[4]

Received: 27 October 2018 / Accepted: 18 February 2019 / Published online: 13 March 2019

Abstract

Thermodynamic and kinetic aspects for the biosorptive removal of Pb, Cd, and Cr metals from water using Chemically Modified Leaves of *Salvia moorcroftiana* (CMSML) were determined. Different parameters including pH, temperature, metal's initial concentration, biomass dosage, and contact time were optimized. Optimum biosorptions of Pb, Cd, and Cr were attained at pH values of 6.0, 7.0, and 3.0 respectively. Batch experiments showed maximum removal of both Pb and Cd at 40 °C and that of Cr at 30 °C. Biosorption capability of CMSML was observed to decrease with raising temperature. Optimal equilibrium times for Pb, Cd, and Cr uptake were 120, 60, and 120 min respectively. Based on the values of regression correlation coefficients (R^2), the current data is explained better by applying Langmuir isotherms than the Freundlich model. Maximum biosorbent capabilities (q_{max}) for Pb, Cd, and Cr were approximately 270.27, 100.00, and 93.45 mg/g respectively. Thermodynamically, removal of all the three metal ions was shown to be exothermic and spontaneous.

Keywords Biosorption · Heavy metals · Batch experiments · Chemical modification · *Salvia moorcroftiana* · Isotherms

Introduction

Rapid industrialization and urbanization have resulted in heavy metal contamination of the terrestrial, aerial, and aquatic environments (Ben Salem et al. 2017; Paschoalini et al. 2019; Wang et al. 2018; Yabanli et al. 2014; Yozukmaz et al. 2018). Different industries including battery manufacturing, metallurgy, fertilizers and agrochemical production, and mining are the major environmental contaminators with hazardous heavy metals (Sdiri et al. 2012). Heavy metals are employed in many industrial processes such as galvanizing, electroplating, tanneries, pigment manufacturing, textile manufacturing, paint productions, and metallurgical processes (Järup 2003; Liu et al. 2010).

The heavy metals Pb, Cd, and Cr are highly toxic and are hazardous to health and the environment of biological systems. The maximum permissible limits of Pb, Cd, and Cr in drinkable water, as recommended by WHO, are 0.010 mg/L (Lalhruaitluanga et al. 2010), 0.005 mg/L (Edris et al. 2014), and 0.005 mg/L (Kozlowski and Walkowiak 2002) respectively. Acute intoxication of humans with Pb adversely affects the gastrointestinal system, central nervous system, kidneys, liver and poses many other health problems (Järup 2003). Accumulation of Cd inside humans causes various acute and chronic ailments such as diarrhea, nausea, pulmonary cramps, salivation, skeletal deformation, renal damage (Leyva-Ramos et al. 2005), hypertensions, emphysema, testicular atrophy, sciatica, liver disease (Bedoui et al. 2008), and carcinogenesis (Brown et al. 2000). Chromium concentration exceeding from permissible limit causes respiratory tract irritation, skin and lung carcinoma, epigastric pain, vomiting (Dearwent et al. 2006; Hayes 1988), and many other diseases.

Being biologically non-destructive, heavy metals persist in the environment and, through food chain, cause hazardous

Responsible editor: Elena Maestri

✉ Syed Muhammad Salman
salman@icp.edu.pk

[1] Department of Chemistry, Islamia College University, Peshawar, Khyber Pakhtunkhwa 25120, Pakistan

[2] Collaborative Innovation Center of Sustainable Energy Materials, Guangxi University, Nanning 530004, People's Republic of China

[3] Pakistan Council of Scientific and Industrial Research (PCSIR) Lab Complex, Jamrud road, Peshawar 25120, Pakistan

[4] Department of Chemistry, Faculty of Sciences, University of Kotli, Kotli, Azad Jammu and Kashmir 11100, Pakistan

effects on both animals' and plants' health. To safeguard biological ecosystems and humans from their adverse health problems, the toxic heavy metals must be removed from industrial effluents before being discharged into the water bodies. Various physicochemical techniques, i.e., ion exchange, membrane filtration, chemical precipitation, electro-dialysis adsorption, and extraction, can be employed for heavy metal removal. However, these techniques have their own inherent limitations. Many of these conventional methods require the use of other chemicals and specialized equipment making them costly for use in small industries. Furthermore, concentration of the resulting sludge and its disposal represents an enormous problem.

In contrast, phytoremediation of polluted water using cheap industrial, agricultural, or urban residues is a promising low-cost alternative. Due to its technical feasibility and low cost, biosorptive detoxification of water is superior to other conventional techniques (Davis et al. 2000; Ben Salem et al. 2017; Yabanli et al. 2014; Yozukmaz et al. 2018).

In the current work, chemically modified leaves of *Salvia moorcroftiana* (CMSML) has been employed as biomass for removal of Pb, Cd, and Cr metals. Metal biosorbing ability of the CMSML was analyzed under various experimental parameters including pH, biosorbent concentration, metal's initial concentration, temperature, and time. The biosorption kinetics was determined using Langmuir and Freundlich models. Furthermore, thermodynamic parameters and utmost biosorption capacity were also determined and compared with other traditionally used sorbents.

Methods and materials

Materials

The reagents HNO_3 (AR 65%), HCl (AR, 38%), and NaOH were purchased from Sigma-Aldrich. The $CaCl_2$ and salts of Pd, Cd, and Cr were purchased from Fluka.

Preparation of biomass and solutions

Leaves of *Salvia moorcroftiana* were collected from Chinagai, Bajaur Agency, Pakistan. The leaves were washed with deionized water and then initially shade dried at ambient temperature and subsequently in electric oven at 46 °C. Dried leaves were powdered and sieved to obtain particles of 44 mesh size. The powder was first treated with 0.1 M HNO_3 for elimination of already contained metals and then with 0.1 M $CaCl_2{\cdot}H_2O$. The chemically treated leaf powder was dried and stored in a desiccator. Stock solutions (1000 ppm) of Pb, Cd, and Cr metals were prepared in deionized water. Working solutions of different concentrations were prepared by diluting appropriate amounts of the stock solution. The pH of working solutions was brought to the desired level using 0.1 M solutions of HCl or NaOH.

Equipment and procedure

All experiments were carried out in temperature-controlled shaker having 16 conical flask clips with an agitation speed of 180 rpm. The effects of various experimental parameters on biosorption were determined through batch biosorption experiments. Each experiment was conducted by treating 100 mL of the test solution with CMSML powder under different conditions of pH (between pH 2.0 and 7.0), biomass dosage (1–30 g/L), metal concentration (20–800 mg/L), time (10–150 min), and temperature (20–50 °C). The CMSML powder was then filtered off with Whatman paper no. 42 and concentrations of the remaining metals in the filtrate were determined by an atomic absorption spectrophotometer. The amount of metals removed by the biosorbent (q_e) and the percent biosorptions were calculated using expressions 1 and 2 respectively:

$$q_e = V \times \frac{(C_o - C_e)}{m} \tag{1}$$

$$\%\ \text{biosorption yield} = \frac{(C_o - C_e)}{C_e} \times 100 \tag{2}$$

where q_e adsorption capacity (mg/g) at equilibrium, and C_o and C_e are equilibrium initial and final concentrations of metal ions in solution, m is mass of biosorbent used, and V is the volume of test solution.

BJH and BET analysis

Pore size, volume, and surface area were analyzed through BJH and BET analysis using NOVA 2000 e model, Quatachrome, USA. Initially, the samples were degassed at pressure of 133.32×10^{-4} Pa for 6 h and then N_2 was adsorbed at 77 K. Total pore volume (V_p) was calculated from volume of nitrogen (as liquid) held at a relative pressure (P/P°) of 0.95.

FT-IR analysis

The FT-IR spectra were recorded at 400–4000 cm^{-1} using a FT-IR spectrometer (ATI Unicam Mattson 1000). A homogenized mixture of the biomass and KBr (1:9 ratios) was compressed to form KBr pellets of 1 mm thickness.

Adsorption kinetics

Adsorption kinetics study gives information about the adsorption mechanism which is very significant for the biosorption efficiency. Pseudo-first-order and pseudo-second-order kinetic models were applied for investigating the adsorption

kinetics. It is important to know the biosorption rate to optimize the parameters (Robinson et al. 2002).

The pseudo-first-order and pseudo-second-order kinetic models were applied using expressions 3 and 4 respectively.

$$\frac{dqt}{dt} = K1(qe-qt) \tag{3}$$

$$\frac{dqt}{dt} = K2(qe-qt)2 \tag{4}$$

where q_t is the adsorption capacity at time t, q_e adsorption capacity at equilibrium, and K_1 is rate constant (1/min) of pseudo-first-order adsorption. K_2 is rate constant (g·min/mg) of pseudo-second-order adsorption.

Adsorption isotherms

Biosorption isotherms explain the interactions between adsorbate molecules and adsorbent surface and therefore Langmuir and Freundlich models were employed (Prasad and Freitas 2000). The Langmuir isotherm model suggests that biosorption is reversible and established only for monolayer on the surface of biosorbent. The isotherm is based on expression 5.

$$qe = \frac{qm\ KL\ Ce}{1} + KLCe \tag{5}$$

where q_e is the mass of the metals biosorbed over adsorbent (mg/g) at equilibrium. C_e is the equilibrium concentration (mg/L), K_L (L/mg) is a constant, and q_m is maximum mass of metals adsorbed per gram of biosorbent (mg/g), which depends on the number of biosorption sites (Kogej et al. 2010).

The Freundlich equation (expression 6) is an empirical model and is applied for a single solute system to explain the distribution process of solute between solid and aqueous states.

$$q_e = K_F\ C_e^{\ 1/n} \tag{6}$$

where $1/n$ and K_F are Freundlich constant ($mg^{1-1/n}\ L^{1/n}\ g^{-1}$) characteristics of the given adsorbent-adsorbate and the temperature. K_F shows the adsorption capacity and n indicates the adsorption energy distribution (Iakovleva and Sillanpää 2013).

Results and discussion

FT-IR analysis

FT-IR spectra of the free and metal loaded CMSML are shown in Fig. 1. The spectrum of unloaded biosorbent (Fig. 1a) indicates the presence of numerous functional groups. The broad

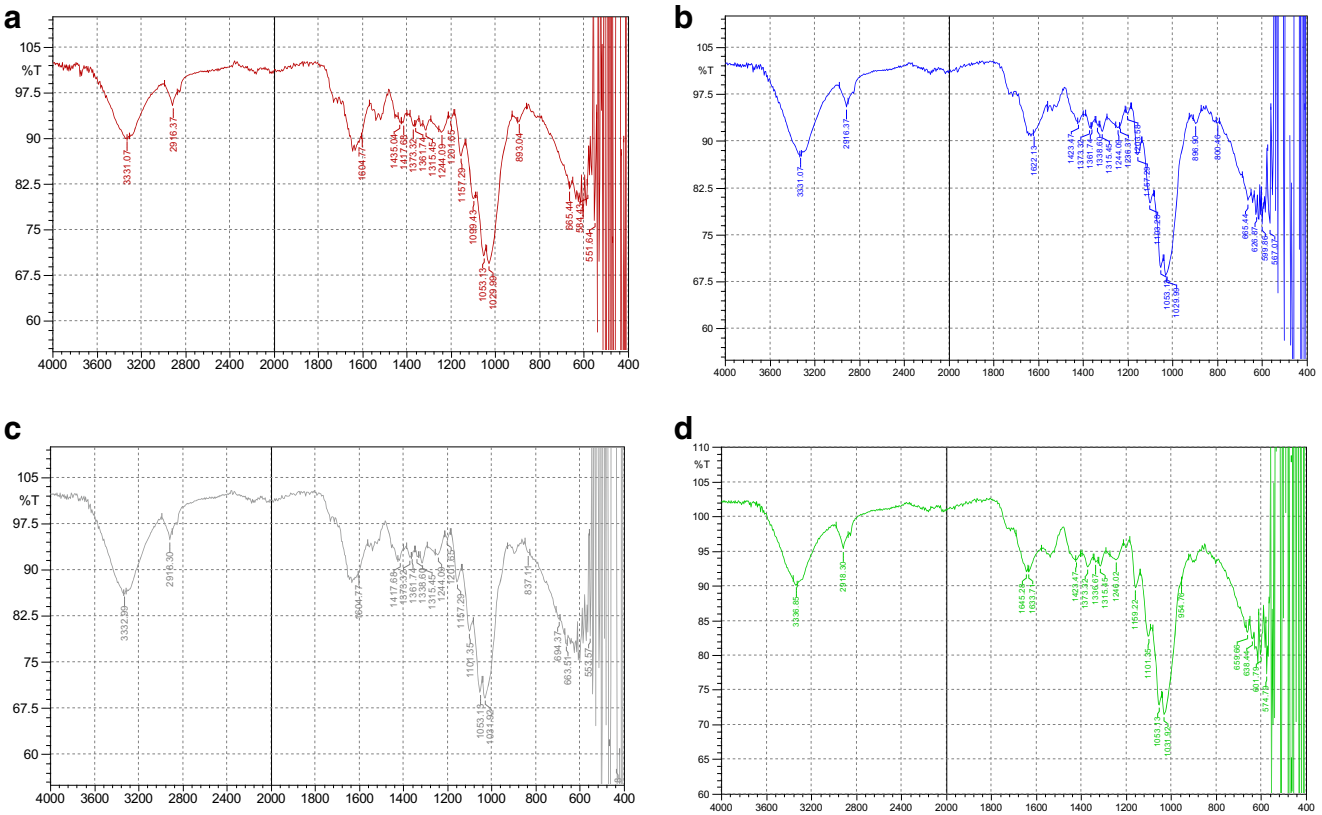

Fig. 1 FT-IR spectra of the biosorbent CMSML (**a**), biosorbent treated with Pb (II) solution (**b**), biosorbent treated with Cd (II) solution (**c**), and biosorbent treated with Cr (VI) solution (**d**)

peak at 3331.07 cm^{-1} shows the stretching of –OH group present to aliphatic compounds (Figueira et al. 1999). The intense and strong band at 1053.13 cm^{-1} is due to C–O stretching indicating the presence of alcoholic groups on biomass surface (Sarı and Tuzen 2008). Absorption peak at 2916.37 cm^{-1} represents C–H stretching of –CH, $–CH_2$ and $–CH_3$ groups. Absorption peak at 1604.77 cm^{-1} indicates C=C stretching of aromatic and alkenes (Figueira et al. 1999). The asymmetrical and symmetrical stretching of C–N were respectively observed at 1315.45 cm^{-1} and 1316.74 cm^{-1} (Sarı and Tuzen 2008). Absorptions at 1435.04 cm^{-1} and 1373.32 cm^{-1} are due to $–CH_3$ and N–H bendings respectively (Tuzen et al. 2009). Most of the functional groups on biosorbent surface have negative charge due to chemical pretreatment and can effectively bind the metal ions (Figueira et al. 1999).

The FT-IR spectra of CMSML treated with metal solutions showed variation in positions and intensities of some peaks. These variations indicate binding interactions between corresponding functional groups and metals. For CMSML treated with Pb (Fig. 1b), the original peak at 1604.77 cm^{-1} was shifted to 1622.13 cm^{-1} showing binding interaction of Pb with C=C group. FT-IR spectrum of CMSML treated with Cd (Fig. 1c) showed slight shifting of the –OH stretching from 3331.07 to 3332.99 cm^{-1}. Treating CMSML with Cd also leads to shifting of –C–H stretching from 2916.37 to 2918.30 cm^{-1}. These changes in absorption frequencies indicate that both the –OH and C–H are involved in the binding of Cd to the biosorbent.

FT-IR spectrum of biosorbent treated with Cr (Fig. 1d) also showed variations in the original absorption frequencies. The peaks located at 3331.07 cm^{-1}, 2916.37 cm^{-1}, and 1604.77 cm^{-1} were shifted respectively to 3336.85 cm^{-1}, 2918.30 cm^{-1}, and 1633.71 cm^{-1} indicating metal binding to these functional groups. A new peak in C=O stretching region was observed at 1645.28 cm^{-1} for CMSML treated with Cr at pH 3.0. This is likely due to oxidation of secondary alcohol to ketone on biosorbent surface by $K_2Cr_2O_7$. Changes in absorption frequencies affirm binding of the Cr with the –CH, –OH, and C=C groups (Yang and Chen 2008).

Table 1 Pore volume, average pore diameter, and surface area of CMSML

Biosorbent	Pore volume (ccg^{-1})	Average pore diameter (A°)	Surface area (BJH) ($m^2\ g^{-1}$)	Surface area (BET) ($m^2\ g^{-1}$)
CMSML	0.95	129.05	285.75	70.07

Scanning electron microscopy

Surface morphologies of natural and chemically modified *Salvia moorcroftiana* leaves were characterized by scanning electron microscopy (SEM). The SEM image of natural *Salvia moorcroftiana* leaves (Fig. 2a) showed a clear morphology. However, after modification and activation, the surface morphology is changed and show irregular edges and crooks (Fig. 2b). The modified surface is appropriate for enhanced metal adsorption (Sarı and Tuzen 2008).

Surface area and pore size analysis

The BET and BJH surface area, pore size, and pore volume were analyzed by surface area and a pore size analyzer. The calculated data are shown in Table 1.

Effect of pH

The ability of hydrogen ions to compete with metal ions for active sites on biomass surface is pH dependent. The effect of altering pH (within pH range 2–7) on biosorption of Pb, Cd, and Cr on CMSML are shown in Fig. 3. The adsorption of Pb and Cd were found to be less at lower pH and was increased with increase in pH. Maximum biosorption of Pb and Cd was observed at pH 6.0 and 7.0 respectively. However, maximum intake of Cr was attained at pH value of 3.0. Biosorption efficiency on different pH conditions can be explained in terms of the availability of functional groups involved binding to metals (Matheickal and Yu 1999).

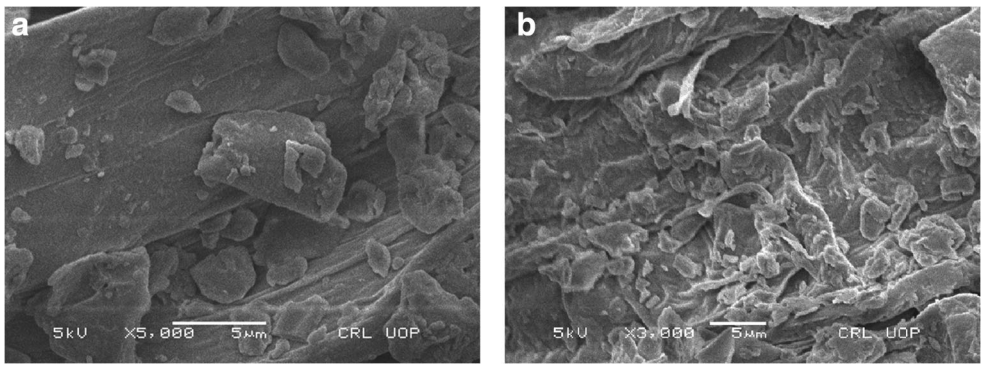

Fig. 2 SEM images of *Salvia moorcroftiana* leaves before modification (**a**) and after modification with HNO_3 and $CaCl_2$ (**b**)

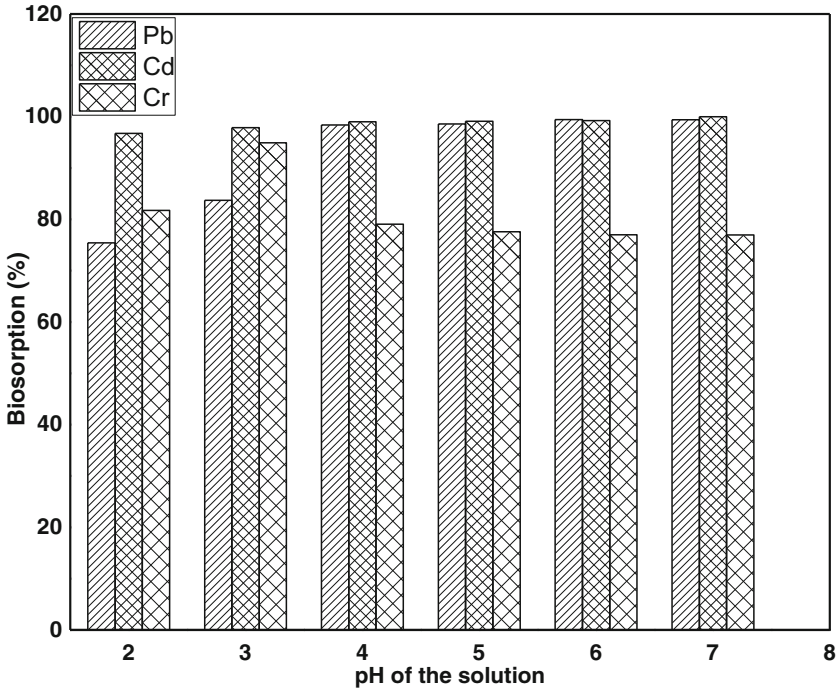

Fig. 3 Effect of pH on biosorption of Pb, Cd, and Cr over CMSML (conditions 100 ppm, 120 min, 0.5 g in 100 mL and 130 rpm)

A plausible mechanism for enhanced biosorptive removal of M^{+2} ions (both Pb (II) and Cd (II)) with increased pH is a substitution of H^+ with M^{+2} on CMSML surface as depicted in expression 7. The driving force for this substitution is the favored coordination between M^{+2} and ligands present on biosorbent surface at high pH.

$$H_2Y^{2-} + M^{2+} \rightleftarrows MY^{2-} + 2H^+ \quad (7)$$

At low pH, the release of H^+ ions from CMSML surface is not favorable and the coordination of M^{2+} is limited. However, high pH was also unfavorable for the coordination of M^{2+} ions because of secondary reaction between M^{2+} and ^-OH ions forming MOH^+ and $M(OH)_2$ predominate. This leads to decreased concentrations of dissolved metal ions and lower competition for the active sites (Rahman and Sathasivam 2015). Unlike Pd and Cd, the maximum biosorption for Cr (VI) occurred at pH 3.0. At low pH, the Cr is predominately in the form of $HCrO_4^-$ ions. Maximum biosorption at lower pH is likely to be favored by more H^+ ions on the CMSML surface leading to strong attraction between positively charged CMSML surface and chromate ions. When the pH is further lowered (pH < 3), the Cr is predominantly present as $H_2Cr_2O_7$ having little affinity towards positively charged CMSML

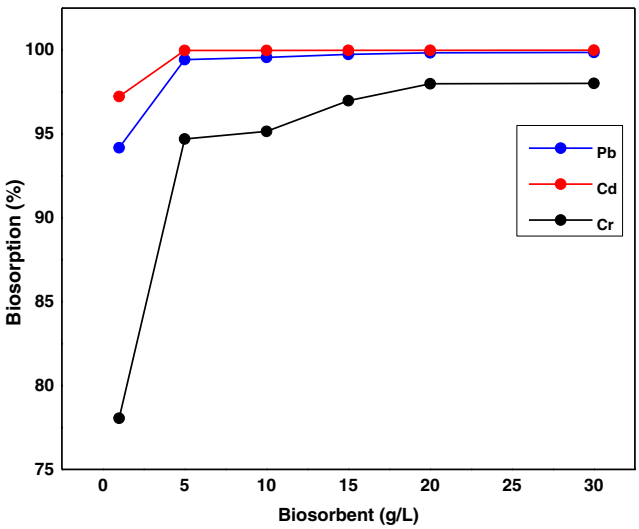

Fig. 4 Effect of biomass dosage on % biosorptions of Pb (II) at pH 5, Cd (II) at pH 7, and Cr (VI) at pH 3, 100 ppm, 120 min, and 130 rpm

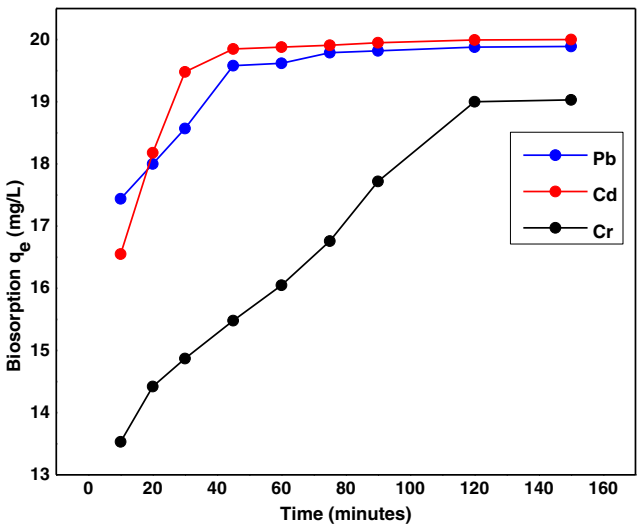

Fig. 5 Equilibrium contact times for Pb, Cd, and Cr biosorption on CMSML at their respective optimal pH conditions (pH 5 for Pb, pH 7 for Cd ions, and pH 3 for Cr), 100 ppm, biomass 0.5 g in 100 mL, 130 rpm

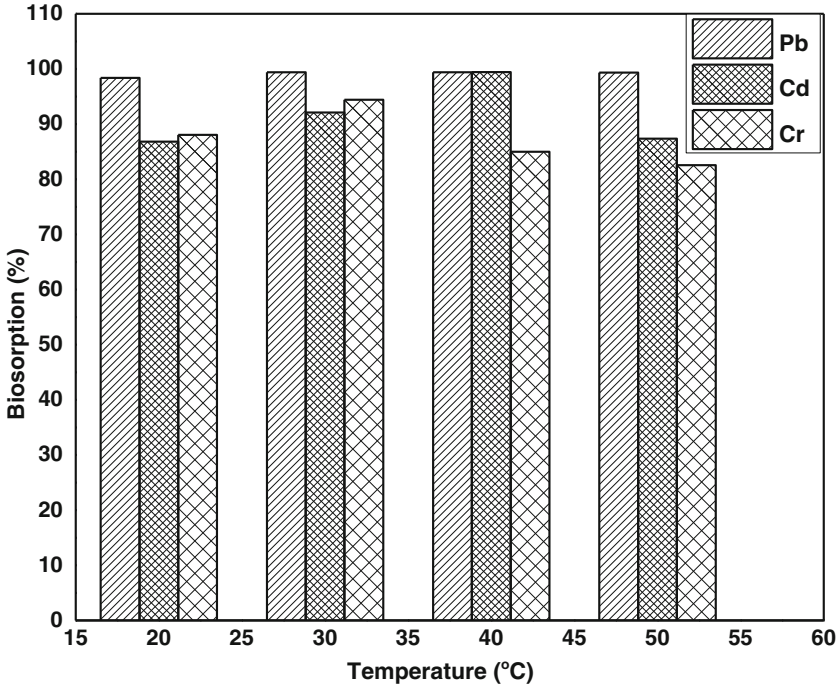

Fig. 6 Effect of temperature on biosorptive removal of Pb, Cd, and Cr over CMSML under optimal conditions of pH and contact times

surface (Lalhruaitluanga et al. 2010). At pH 6 and above, competitive coordination of both ^{-}OH and CrO_4^{2-} ions with CMSML surface predominates and biosorptions of Cr is not of practical significance (Pagnanelli et al. 2003).

Effect of biosorbent dosage

The effects of biosorbent dosage on biosorption potency are shown in Fig. 4. Percent uptake of all the three metals was observed to increases with biomass loading of up to 5 g/L. For Pb and Cd, the maximum percent biosorptions (99.44% and 99.97% respectively) were attained at biosorbent dosage of 5 g/L and remained persistent at higher dosages. For Cr, drastic increase in % biosorption was observed at dosages up to 5 g/L. Further increase in biosorbent dosage led to a slight increase until the maximum % biosorption (97.99%) was attained at a dosage of 20 g/L. The persistence of % biosorption at higher dosages is due to partial aggregation of biosorbent, decreasing effective surface area for metal biosorption (Barka et al. 2008; Karthikeyan et al. 2007).

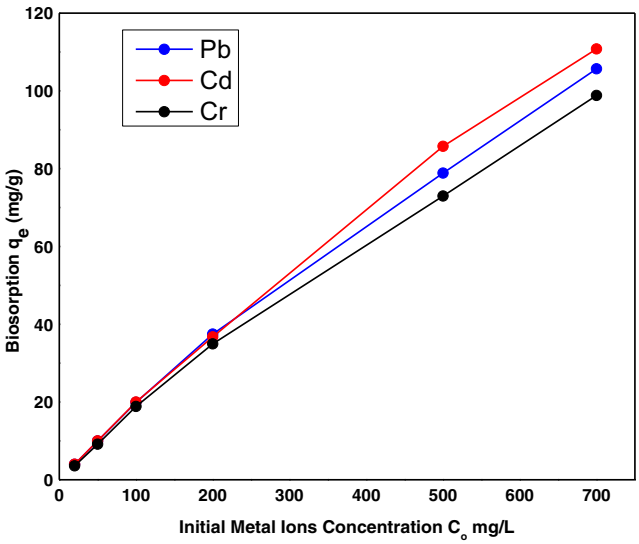

Fig. 7 Effect of tested metal concentrations on biosorption over CMSML under their respective optimal conditions of pH, dosage, and time

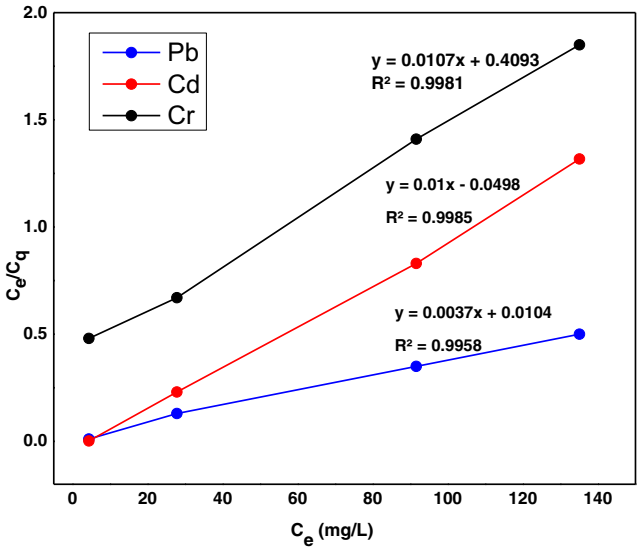

Fig. 8 Langmuir plots for biosorption of Pd, Cd, and Cr metal ions

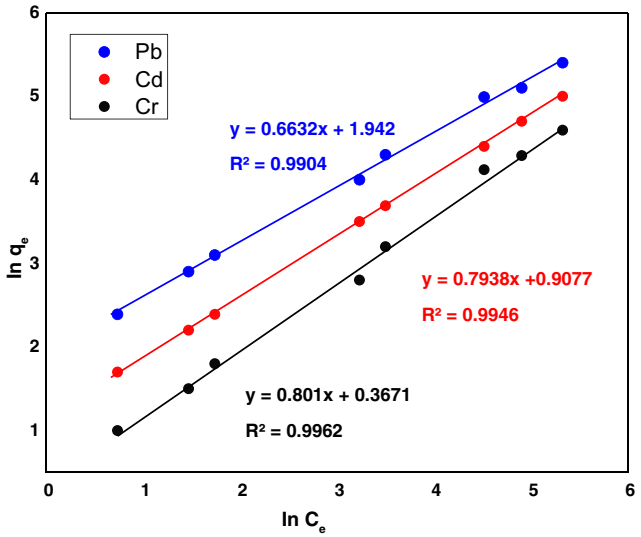

Fig. 9 Freundlich plots for biosorption of Pd, Cd, and Cr metal ions

Effect of contact time

The influence of contact time on biosorbing capacity as determined is shown in Fig. 5. Contact time was found to affect biosorption capacity of CMSML significantly and the biosorption yield of all the tested metal ions increases with increase in contact time up to 120 min. Biosorption of both Pd and Cd increased significantly for initial contact time of 40 min and negligible increase was observed on further extension of contact time. For Cr, the biosorption capacity kept on increasing until attainment of maximum capacity at 120 min. The optimized time for further experiments was chosen as 120 min (Gong et al. 2005).

Effect of temperature

The effect of temperatures between 20–50 °C on metal uptake by CMSML is shown in Fig. 6. A decrease in metal uptake was observed with increasing temperature. This is apparently due to damage of the active coordination sites in the biosorbent (Özer and Özer 2003), and due to increasing desorption of the metals from interface into solution (Saltalı et al. 2007). The biosorbent surface has several binding sites and each site can be affected by changing temperature (Aksu and Tezer 2000). For Cd, the biosorption increased up to 40 °C and then acquired decreasing trend on further temperature rise. Uptake of Cr increased up to 30 °C and declined with further rise in temperature. Maximum uptake of Pd and Cd took place at 40 °C while that of Cr at 30 °C.

Effect of initial metal ion concentration

Biosorption as a function of metal concentrations was determined by varying initial concentrations of Pb, Cd, and Cr between 20 and 800 mg/L (Fig. 7). The results indicated that by raising the metal concentration, the capability of biosorbent to eliminate the metals increased but percent biosorption was decreased. Although, at higher concentrations, the number of metal ions is more than the available binding sites; however, intraparticle diffusion of the ions on biomass surface leads to a decrease in percent biosorption (Azizi et al. 2016).

Biosorption isotherm models

The Langmuir and Freundlich isotherm models were applied to investigate the probable mechanism of metal biosorption to the CMSML. The Langmuir model predicts monolayer biosorption on homogenous surface having no interaction with biosorbed molecules. However, the model also explains uniform energies of biosorption on the surface and no transmigration of the adsorbate. Langmuir equation is given as (Langmuir 1918)

$$\frac{Ce}{qe} = \frac{Ce}{qm} + \frac{1}{KL\ qm} \tag{8}$$

where q_e is the equilibrium concentration of metal ions onto biomass (mg/g), C_e is the equilibrium of metals in solution (mg/L), q_m is the biosorption monolayer capability of the biomass (mg/g), and K_L is Langmuir constant (L/mg).

A linear relationship was depicted between ratio of Ce/qe and concentrations of metals in solution (Fig. 8). The regression correlation coefficients (R^2) showing metal uptake onto CMSML properly followed the Langmuir model. Generally, the isotherm plot indicated enhancement of the biosorption capacity with initial concentration of metal until the surface of CMSML reached saturation. Maximum biosorption potencies (q_m) of CMSML were determined to be 136.99 mg/g for Pb, 112.36 mg/g for Cd, and 90.91 mg/g for Cr. The K_L(b) values for Pb, Cd, and Cr ions were found to be 0.258 L/mg, 0.0813 L/mg, and 0.028 L/mg respectively. The Freundlich isotherm

Table 2 Adsorption isotherm constants for CMSML-mediated biosorptive removal of Pd, Cd, and Cr ions

Metal ions	Langmuir			Freundlich		
	q_{max} (mg/g)	K_L (L/mg)	R^2	n (g/L)	K_F (L/g)	R^2
Pb (II)	270.27	0.356	0.9985	1.507	6.97	0.9904
Cd (II)	100	0.200	0.9985	1.2597	2.47	0.9946
Cr (IV)	93.45	0.026	0.9981	1.248	1.44	0.9962

model, expression 9, explains a monolayer biosorption with a heterogeneous distribution of energetic active sites and strong interactions between biosorbed substances (Freundlich 1907).

$$\log qe = \log KF + \frac{1}{n}\log Ce \quad (9)$$

wherein K_f is Freundlich constant of biosorption potential and $1/n$ is a characteristic empirical parameter relevant to the intensity of biosorption. The Freundlich isotherm plots for biosorptive removal of Pb, Cr, and Cr over CMSML are shown in Fig. 9. The K_F and $1/n$ values calculated for Pb (II), Cd (II), and Cr (IV) were found to be 25.62 and 2.36, 18.47 and 2.97, and 3.64 and 1.57 respectively. The values of $1/n$ vary from 0 to 1 demonstrating favorable biosorption of all metal ions. The R^2 values calculated for Pb, Cd, and Cr were 0.998, 0.988, and 0.933 respectively (Table 2).

A comparison of the biosorption capacity of CMSML with other reported biosorbents for the removal of Pd, Cd, and Cr ions is given in Table 3. CMSML possess higher biosorption capacity than majority of the reported biosorbents suggesting CMSML to be a superior biosorbent for water detoxification.

Biosorption kinetics

To determine the kinetics of CMSML-mediated biosorptive removal of Pd, Cd, and Cr, pseudo-first-order and pseudo-second-order kinetic models were plotted to the findings.

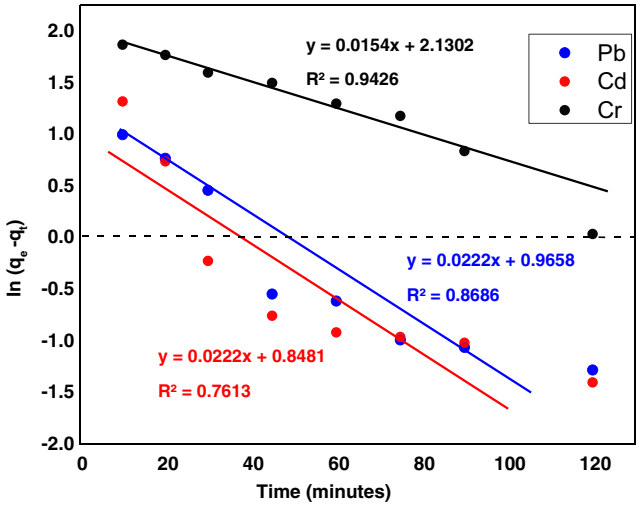

Fig. 10 Plots obtained for metal biosorptions after applying pseudo-first-order kinetic model

Linear rate equation for the pseudo-first-order of Langergren is given (Lagergren 1898).

$$\ln (q_e - q_t) = \ln q_e - K_1 t \quad (10)$$

where q_t and q_e are the biosorption capabilities (mg/g) at time t and at equilibrium and k_1 is the kinetic rate constant. The kinetic rate constant can be explained experimentally by plotting $\ln (q_e - q_t)$ versus t for pseudo-first-order equation as given in Fig. 10. The determination of regression correlation

Table 3 Comparison of biosorption capacity (mg/g) of CMSML with other reported biosorbents for the removal of Pb, Cd, and Cr

Biosorbent	Pb (II)		Cd (II)		Cr (VI)		References
	q_{max}	pH	q_{max}	pH	q_{max}	pH	
Ulva lactuca	34.7	5.0	29.2	6.0			Sarı and Tuzen (2008)
Cephalosporium aphidicola	36.9	5.0	–	–	–	–	Tunali et al. (2006)
Phanerochaete chrysosporium	69.8	6.0	23.0	6.0			Say et al. (2001)
Rhizopus arrhizus	15.5	5.0	–	–	–	–	Sağ et al. (1995)
Phellinus badius	170	5.0	–	–	–	–	Matheickal and Yu (1997)
Zoogloea ramigera	10.4	4.5	–	–	–	–	Sağ et al. (1995)
Aspergillus flavus	13.5	5.0	–	–	–	–	Akar and Tunali (2006)
Mucor rouxii	–	–	20.3	6.0	–	–	Yan and Viraraghavan (2003)
Rhizopus arrhizus	–	–	26.8	6–7	–	–	Fourest and Roux (1992)
Phanerochaete chrysosporium	–	–	15.2	4.5	–	–	Li et al. (2004)
Streptomyces longwoodensis	100.0	3.0	–	–	–	–	Friis and Myers-Keith (1986)
Streptomyces noursei	–	–	3.4	6.0	–	–	Mattuschka and Straube (1993)
Salvia cucullata	–	–	–	–	159.2	1.7	Baral et al. (2009)
Modeified corn stalk	–	–	–	–	102	2.6	Chen et al. (2012)
Quercus ithaburensis	–	–	–	–	62.76	2.0	Malkoc et al. (2006)
Savia moorcroftiana	136.99	6.0	112.45	7.0	90.90	3.0	Present study

Table 4 Kinetic parameters obtained from pseudo-first-order and pseudo-second-order kinetic models for biosorption of Pb, Cd, and Cr onto CMSML

Metals	Pseudo-first order			Pseudo-second order		
	K_1 (1/min)	q_{e1} (mg/g)	R^2	K_2 (g/mg min)	q_{e2} (mg/g)	R^2
Pb (II)	0.00051	45.045	0.8686	0.028	20.162	0.999
Cd (II)	0.00058	45.045	0.7613	0.032	20.284	0.999
Cr (VI)	0.00011	64.930	0.9426	4.878	20.040	0.994

coefficients R^2 is low, as shown in Table 4. From the values of R^2, it can be deduced that the biosorption of all the three metals do not follow the pseudo-first-order kinetic model (Sari et al. 2008). The findings were also evaluated by pseudo-second-order kinetic model using Eq. 11. (Ho and McKay 1999)

$$\frac{1}{qt} = \frac{1}{K2\ qe2} + \left(\frac{1}{qe}\right)t \tag{11}$$

where K_2 (g·mg^{-1} min^{-1}) is the rate constant for pseudo-second-order process, q_t (mg/g) is the biosorption mass at time t, and q_e is the biosorbed amount (mg/g) at equilibrium. This kinetic model is likely to point out kinetic behavior of biosorption of heavy metals with chemical sorption being the controlling step of reaction rate (Ho and McKay 2000). The linear plots of the ratio (t/qt) versus t for the pseudo-second-order kinetic model at 20 to 50 °C are presented in Fig. 11. The rate constants K_2, the value of R^2, and the values of q_e are presented in Table 4. The regression correlation coefficient R^2 values were very large for the biosorption of the tested metals. The biosorptions of Pb (II), Cd (II), and Cr (IV) ions onto CMSML were found to be well in compliance with

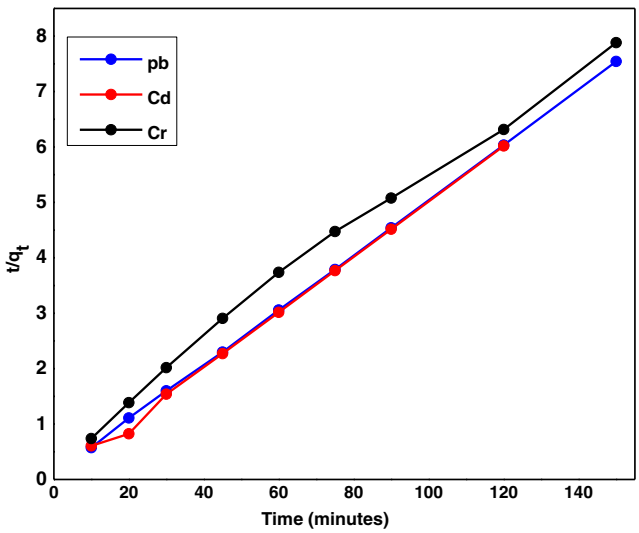

Fig. 11 Plots obtained for metal biosorptions after applying pseudo-second-order kinetic model

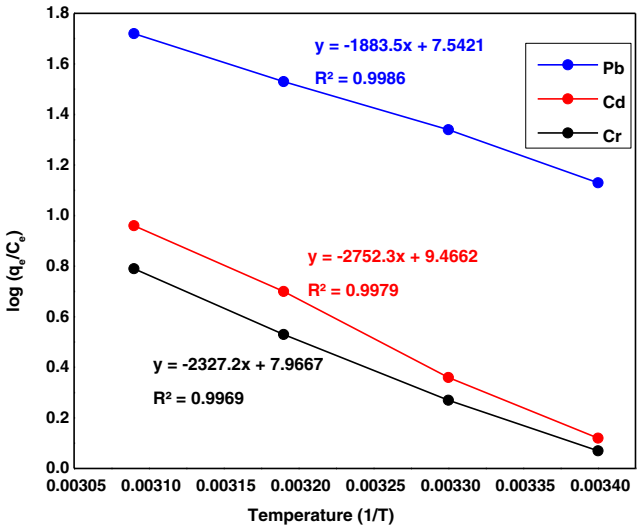

Fig. 12 Van't Hoff's plot for CMSML-mediated biosorptive uptake of Pd, Cd, and Cr

the pseudo-second-order kinetic model (Farhan et al. 2013).

Thermodynamic aspects

Thermodynamic parameters including standard enthalpy changes (ΔH°), standard change in Gibbs free energy (ΔGo°), and standard changes in entropy (ΔS°) for biosorptive removal of test metals through CMSML were determined using Eqs. 12 and 13.

$$\Delta G^{\circ} = -RT \ln K_D \tag{12}$$

where R is the universal gas constant, K_D (q_e/C_e) is the distribution coefficient, and T is temperature in Kelvin (Sawalha et al. 2006). The standard enthalpies (H°) and entropies (S°) were calculated using the following equation:

$$\ln KD = \frac{\Delta S0}{R} - \frac{\Delta H0}{RT} \tag{13}$$

The parameters $S°$ and $H°$ were deduced from the intercept and slope of the plot of ln K_D vs $1/T$ yields, respectively and were shown in Fig. 12. The negative ΔG° values calculated for metal uptake in Table 5 show biosorptive removal of the tested metals to be spontaneous and thermodynamically feasible. The negative ΔH° for biosorptions of all the three tested

Table 5 Thermodynamic parameters for biosorption of Pd, Cd, and Cr

Metals	ΔH° (KJmol^{-1})	ΔS° (Jmol^{-1} K^{-1})	ΔG° (KJmol^{-1})			
			298 K	303 K	313 K	323 K
Pb	−36.06	0.144	−78.97	−79.69	−81.13	−82.57
Cd	−52.69	0.181	−106.62	−107.53	−109.34	−111.15
Cr	−44.55	0.152	−89.84	−90.60	−92.12	−93.64

metals indicates the process to be exothermic at 298–323 K. The positive values of ΔS^0 indicate that biosorptions were favorable (Singh et al. 2006).

Conclusions

Current study explored different experimental, kinetic, and thermodynamic aspects of the use of chemically modified *Salvia moorcroftiana* leaves (CMSML) for biosorptive detoxification of aqueous solutions by removing Pb (II), Cd (II), and Cr (IV) ions. The batch biosorption parameters were shown to affect the biosorption potency of CMSML. Biosorption potencies of CMSML for Pb (II), Cd (II), and Cr (IV) ions were 270.27 mg g^{-1}, 100 mg g^{-1}, and 93.90 mg g^{-1} respectively. FT-IR spectra indicated changes in absorption frequencies of different groups due to metal-ligand binding. At biomass dosage of 5 g, optimum conditions for effective elimination of Pb (II), Cd (II), and Cr (IV) are pH 6.0, 7.0, and 3.0, contact time 120 min, 60 min, and 120 min, temperature 40 °C, 40 °C, and 30 °C, respectively. Kinetic studies indicated that the removal of Pb (II), Cd (II), and Cr (IV) ions onto CMSML obeys the pseudo-second-order kinetics. Thermodynamic studies revealed that the biosorptions of both Pb (II) and Cd (II) ions are spontaneous and exothermic, while that of Cr (IV) ions are endothermic and non-spontaneous. Due to its high biosorption potency and low cost, *Salvia moorcroftiana* can be considered good alternative to other biosorbents for detoxification of water contaminated with Pb (II), Cd (II), and Cr (IV) ions.

References

Akar T, Tunali S (2006) Biosorption characteristics of *Aspergillus flavus* biomass for removal of Pb (II) and Cu (II) ions from an aqueous solution. Bioresour Technol 97:1780–1787

Aksu Z, Tezer S (2000) Equilibrium and kinetic modelling of biosorption of Remazol Black B by Rhizopus arrhizus in a batch system: effect of temperature. Process Biochem 36:431–439

Azizi S, Kamika I, Tekere M (2016) Evaluation of heavy metal removal from wastewater in a modified packed bed biofilm reactor. PLoS One 11:e0155462

Baral S, Das N, Ramulu T, Sahoo S, Das S, Chaudhury GR (2009) Removal of Cr (VI) by thermally activated weed *Salvinia cucullata* in a fixed-bed column. J Hazard Mater 161:1427–1435

Barka N, Qourzal S, Assabbane A, Nounah A, Yhya A-I (2008) Adsorption of disperse blue SBL dye by synthesized poorly crystalline hydroxyapatite. J Environ Sci 20:1268–1272

Bedoui K, Bekri-Abbes I, Srasra E (2008) Removal of cadmium (II) from aqueous solution using pure smectite and Lewatite S 100: the effect of time and metal concentration. Desalination 223:269–273

Ben Salem Z, Laffray X, Al-Ashoor A, Ayadi H, Aleya L (2017) Metals and metalloid bioconcentrations in the tissues of *Typha latifolia* grown in the four interconnected ponds of a domestic landfill site. J Environ Sci (China) 54:56–68

Brown P, Gill S, Allen S (2000) Metal removal from wastewater using peat. Water Res 34:3907–3916

Chen S, Yue Q, Gao B, Li Q, Xu X, Fu K (2012) Adsorption of hexavalent chromium from aqueous solution by modified corn stalk: a fixed-bed column study. Bioresour Technol 113:114–120

Davis T, Volesky B, Vieira R (2000) Sargassum seaweed as biosorbent for heavy metals. Water Res 34:4270–4278

Dearwent SM, MUMTAZ M, Godfrey G, Sinks T, Falk H (2006) Health effects of hazardous waste. Ann N Y Acad Sci 1076:439–448

Edris G, Alhamed Y, Alzahrani A (2014) Biosorption of cadmium and lead from aqueous solutions by *Chlorella vulgaris* biomass: equilibrium and kinetic study. Arab J Sci Eng 39:87–93

Farhan AM, Al-Dujaili AH, Awwad AM (2013) Equilibrium and kinetic studies of cadmium (II) and lead (II) ions biosorption onto *Ficus carcia* leaves. International Journal of Industrial Chemistry 4:24

Figueira M, Volesky B, Mathieu H (1999) Instrumental analysis study of iron species biosorption by Sargassum biomass. Environ Sci Technol 33:1840–1846

Fourest E, Roux J-C (1992) Heavy metal biosorption by fungal mycelial by-products: mechanisms and influence of pH. Appl Microbiol Biotechnol 37:399–403

Freundlich H (1907) Über die adsorption in lösungen. Z Phys Chem 57: 385–470

Friis N, Myers-Keith P (1986) Biosorption of uranium and lead by *Streptomyces longwoodensis*. Biotechnol Bioeng 28:21–28

Gong R, Ding Y, Li M, Yang C, Liu H, Sun Y (2005) Utilization of powdered peanut hull as biosorbent for removal of anionic dyes from aqueous solution. Dyes Pigments 64:187–192

Hayes RB (1988) Review of occupational epidemiology of chromium chemicals and respiratory cancer. Sci Total Environ 71:331–339

Ho Y-S, McKay G (1999) Pseudo-second order model for sorption processes. Process Biochem 34:451–465

Ho Y-S, McKay G (2000) The kinetics of sorption of divalent metal ions onto sphagnum moss peat. Water Res 34:735–742

Iakovleva E, Sillanpää M (2013) The use of low-cost adsorbents for wastewater purification in mining industries. Environ Sci Pollut Res 20:7878–7899

Järup L (2003) Hazards of heavy metal contamination. Br Med Bull 68: 167–182

Karthikeyan S, Balasubramanian R, Iyer C (2007) Evaluation of the marine algae Ulva fasciata and Sargassum sp. for the biosorption of Cu (II) from aqueous solutions. Bioresour Technol 98:452–455

Kogej A, Likozar B, Pavko A (2010) Lead biosorption by self-immobilized Rhizopus nigricans pellets in a laboratory scale packed bed column: mathematical model and experiment. Food Technol Biotechnol 48

Kozlowski CA, Walkowiak W (2002) Removal of chromium (VI) from aqueous solutions by polymer inclusion membranes. Water Res 36: 4870–4876

Lagergren S (1898) Zur theorie der sogenannten adsorption geloster stoffe, Kungliga svenska vetenskapsakademiens. Handlingar 24:1–39

Lalhruaitluanga H, Jayaram K, Prasad M, Kumar K (2010) Lead (II) adsorption from aqueous solutions by raw and activated charcoals of Melocanna baccifera Roxburgh (bamboo)—a comparative study. J Hazard Mater 175:311–318

Langmuir I (1918) The adsorption of gases on plane surfaces of glass, mica and platinum. J Am Chem Soc 40:1361–1403

Leyva-Ramos R, Diaz-Flores PE, Aragon-Piña A, Mendoza-Barron J, Guerrero-Coronado RM (2005) Adsorption of cadmium (II) from an aqueous solution onto activated carbon cloth. Sep Sci Technol 40: 2079–2094

Li Q, Wu S, Liu G, Liao X, Deng X, Sun D, Hu Y, Huang Y (2004) Simultaneous biosorption of cadmium (II) and lead (II) ions by pretreated biomass of Phanerochaete chrysosporium. Sep Purif Technol 34:135–142

Liu Y, Sun X, Li B (2010) Adsorption of Hg^{2+} and Cd^{2+} by ethylenediamine modified peanut shells. Carbohydr Polym 81: 335–339

Malkoc E, Nuhoglu Y, Abali Y (2006) Cr (VI) adsorption by waste acorn of Quercus ithaburensis in fixed beds: prediction of breakthrough curves. Chem Eng J 119:61–68

Matheickal J, Yu Q (1997) Biosorption of lead (II) from aqueous solutions by Phellinus badius. Miner Eng 10:947–957

Matheickal JT, Yu Q (1999) Biosorption of lead (II) and copper (II) from aqueous solutions by pre-treated biomass of Australian marine algae. Bioresour Technol 69:223–229

Mattuschka B, Straube G (1993) Biosorption of metals by a waste biomass. J Chem Technol Biotechnol 58:57–63

Özer A, Özer D (2003) Comparative study of the biosorption of Pb (II), Ni (II) and Cr (VI) ions onto S. cerevisiae: determination of biosorption heats. J Hazard Mater 100:219–229

Pagnanelli F, Esposito A, Toro L, Veglio F (2003) Metal speciation and pH effect on Pb, Cu, Zn and Cd biosorption onto Sphaerotilus natans: Langmuir-type empirical model. Water Res 37:627–633

Paschoalini AL, Savassi LA, Arantes FP, Rizzo E, Bazzoli N (2019) Heavy metals accumulation and endocrine disruption in Prochilodus argenteus from a polluted neotropical river. Ecotoxicol Environ Saf 169:539–550

Prasad M, Freitas H (2000) Removal of toxic metals from solution by leaf, stem and root phytomass of Quercus ilex L. (holly oak). Environ Pollut 110:277–283

Rahman MS, Sathasivam KV (2015) Heavy metal adsorption onto Kappaphycus sp. from aqueous solutions: the use of error functions for validation of isotherm and kinetics models. Biomed Res Int 2015:13

Robinson T, Chandran B, Nigam P (2002) Removal of dyes from a synthetic textile dye effluent by biosorption on apple pomace and wheat straw. Water Res 36:2824–2830

Sağ Y, Özer D, Kutsal T (1995) A comparative study of the biosorption of lead (II) ions to Z. ramigera and R. arrhizus. Process Biochem 30: 169–174

Saltalı K, Sarı A, Aydın M (2007) Removal of ammonium ion from aqueous solution by natural Turkish (Yıldızeli) zeolite for environmental quality. J Hazard Mater 141:258–263

Sarı A, Tuzen M (2008) Biosorption of Pb (II) and Cd (II) from aqueous solution using green alga (Ulva lactuca) biomass. J Hazard Mater 152:302–308

Sari A, Mendil D, Tuzen M, Soylak M (2008) Biosorption of Cd (II) and Cr (III) from aqueous solution by moss (Hylocomium splendens) biomass: equilibrium, kinetic and thermodynamic studies. Chem Eng J 144:1–9

Sawalha MF, Peralta-Videa JR, Romero-González J, Gardea-Torresdey JL (2006) Biosorption of Cd (II), Cr (III), and Cr (VI) by saltbush (Atriplex canescens) biomass: thermodynamic and isotherm studies. J Colloid Interface Sci 300:100–104

Say R, Denizli A, Arıca MY (2001) Biosorption of cadmium (II), lead (II) and copper (II) with the filamentous fungus Phanerochaete chrysosporium. Bioresour Technol 76:67–70

Sdiri A, Higashi T, Jamoussi F, Bouaziz S (2012) Effects of impurities on the removal of heavy metals by natural limestones in aqueous systems. J Environ Manag 93:245–253

Singh K, Singh A, Hasan S (2006) Low cost bio-sorbent 'wheat bran' for the removal of cadmium from wastewater: kinetic and equilibrium studies. Bioresour Technol 97:994–1001

Tunali S, Akar T, Özcan AS, Kiran I, Özcan A (2006) Equilibrium and kinetics of biosorption of lead (II) from aqueous solutions by Cephalosporium aphidicola. Sep Purif Technol 47:105–112

Tuzen M, Sari A, Mendil D, Soylak M (2009) Biosorptive removal of mercury (II) from aqueous solution using lichen (Xanthoparmelia conspersa) biomass: kinetic and equilibrium studies. J Hazard Mater 169:263–270

Wang M, Liu R, Chen W, Peng C, Markert B (2018) Effects of urbanization on heavy metal accumulation in surface soils, Beijing. J Environ Sci 64:328–334

Yabanli M, Yozukmaz A, Sel F (2014) Heavy metal accumulation in the leaves, stem and root of the invasive submerged macrophyte Myriophyllum spicatum L. (Haloragaceae): an example of Kadin Creek (Mugla, Turkey). Braz Arch Biol Technol 57:434–440

Yan G, Viraraghavan T (2003) Heavy-metal removal from aqueous solution by fungus Mucor rouxii. Water Res 37:4486–4496

Yang L, Chen JP (2008) Biosorption of hexavalent chromium onto raw and chemically modified Sargassum sp. Bioresour Technol 99:297–307

Yozukmaz A, Yabanli M, Sel F (2018) Heavy metal bioaccumulation in Enteromorpha intestinalis, (L.) Nees, a macrophytic algae: the example of Kadin Creek (Western Anatolia). Braz Arch Biol Technol 61